JETIR.ORG ISSN: 2349-5162 | ESTD Year : 2014 | Monthly Issue
JOURNAL OF EMERGING TECHNOLOGIES AND INNOVATIVE RESEARCH (JETIR)
An International Scholarly Open Access, Peer-reviewed, Refereed Journal

An Investigation on Torsional Behaviour of Recycled Aggregate Based Steel Fiber Reinforced Self-Compacting Concrete

[1]Muntzir Mehdi, Mtech (Civil Engineering), Institute of Technology and Management Lucknow
[2]Mr. Shakti Kumar, Assistant Professor, Department of Civil Engineering, Bansal Institute of Engineering and Technology, Lucknow

Abstract : The strength and durability of concrete depend critically on the quality of its compaction. Self-Compacting Concrete eliminates the need for vibrating equipment since it naturally achieves consolidation. There is still much to learn about its behaviour, particularly in torsion, which is only one of several areas that require attention. Torsion is a fundamental structural motion that is often overlooked yet crucial when examining buildings exposed to wind and seismic forces. When studying buildings exposed to lateral forces, the torsional stiffness, toughness, and twist at ultimate torque of a part are crucial. Incorporating steel fibres into concrete improves its ability to absorb impact force. A more eco-friendly concrete may be made from recycled aggregates. Torsional behaviour of steel fibre reinforced recycled aggregate based Self-compacting concrete has received little attention in the literature.

Index Terms **- SCC mixes self-compacting concrete, Beam-Column Joint, Loading Arrangement, Behaviour and Failure Mechanisms**

1.1 Introduction

Axial compression, tension, bending moment, shear force, and torsional moment are the five fundamental actions that may be used to characterise any complicated force system. Space frames, inverted L-beams for supporting sunshades, curved beams for water tanks, edge beams of slab, spandrel beams, etc. are all examples of structural components where torsion plays a significant role. Structural analysis of torsion in reinforced beams is notoriously difficult. The more difficult to solve issue of torsion in reinforced concrete members may be better grasped by conducting torsion tests on plain concrete members. Research of reinforced concrete is not necessary before reading this. Adding steel fibres to simple concrete members explains their improved torsion resistance [1]. Concrete is often regarded as the most adaptable building material. The strength and longevity of the hardened characteristics are compromised by poor compaction. Consolidation may be achieved using self-compacting concrete without the use of vibrating equipment, eliminating a major source of delay in construction. SCC may be used to completely fill the formwork without any segregation or loss of integrity, and it can keep its homogeneity even in reinforcing hotspots. Torsional strength in a reinforced concrete member is often just a small percentage of that in an equivalent plain concrete member. The construction industry may save money, time, and energy by using recycled concrete aggregates (RCA) in structural concrete (SCC). With the rising demand for building materials throughout the world, recycling concrete and asphalt offers a viable option that may have positive effects on both the environment and the bottom line. Due to the high need for alternatives, recycled aggregates derived from destroyed structures are seeing widespread application. Fibers added to recycled concrete aggregates increase the material's durability and energy absorption capability. There has been a lack of research on these factors when considering SCC in a torsional environment. In light of the dearth of information on how to build a mix for SCC, developed a straightforward mix design approach for SCC, in which the term "Packing Factor" was created to determine the required amounts of aggregates. As part of the procedure, we calculated the aggregate Packing Factor (PF) and its effect on the material's strength, flowability, and self-compatibility. SCC Requirements and Procedures Material specifications, composition, and usage for SCC are all defined by EFNARC. Several tests were suggested by EFNARC recommendations to describe the new qualities of SCC, such as its flowability, passing ability, viscosity, and segregation resistance. It was hypothesised that by using large amounts of Class F fly ash in SCC mixtures, it would be possible to reduce production costs [2]. The resistance of fibres to torsional stresses in vibrated concrete was investigated. Steel fibre reinforced concrete beams were researched, who came to the same conclusion: that the torsional characteristics of plain beams improve with an increase in the concrete tensile strength when steel fibres are included into the mix. Hookend fibre greatly impact post peak behaviour of SCC compared to straight fibres, according to researched. The structural behaviour and fracture energy of steel-fiber-reinforced concrete may be enhanced by using a sustainable material. According to study Self-compacting concrete using recycled coarse aggregate produced from crushed concrete, as investigated by researcher. The findings showed that there is only a little change in the qualities of these concretes, suggesting that recycled coarse aggregate might be utilised effectively in the production of self-compacting concrete. In both pure torsion and mixed bending and torsion, the load-carrying capacity of concrete is increased by the addition of steel fibres. A research on the strength properties of recycled coarse aggregate with several replacement levels and found that a 25% replacement level would not appreciably alter the strength characteristics. Evaluated the performance of vibrated concrete (VC) with 100% natural aggregate to determine the effect of varying proportions of recycled coarse aggregate (RCA) derived from a demolished waste on the qualities of self-compacting concrete (SCC) (NA). According to the findings, using RA as a substitute for 30% of the SCC nearly fully met the specified compressive strength. After reading up on SCC, it became clear that this novel material is capable of self-compacting into all the nooks and crannies of the formwork. Numerous books and articles have been written on SCC [3]. Especially in SCC, the use of recycled materials to substitute natural aggregates in concrete is gaining popularity. Based on the research conducted, it was determined that using recycled aggregates as a replacement for natural aggregates is an efficient means of dealing with the disposal of waste concrete, provided that the appropriate replacement proportions are employed. However, there is a dearth of information on the torsional behaviour of steel fibre reinforced SCC in the literature. The research was conducted in two parts. To achieve the ideal proportion of SCC mixture, RBA and steel FIBERs were used to partly replace natural aggregates in the first step. To achieve this goal, many permutations were tried. The second stage of this experimental programme entails testing miniature versions of the external beam-column connection.

1.2 Development of SCC Mixes

The optimal development of the SCC blends required resolving a pair of contrasting problems. For one, the SCC must keep its maximum degree of fluidity, and for another, it must remain stable to prevent the segregation of solids. An SP may help keep the solids-to-liquids ratio in check when employing sand as a reinforcing element in concrete [4]. Workability issues need determining the optimal amount of steel FIBERs to provide minimum loss of workability while maintaining sufficient flow and passing ability. This is how SCC mixtures came to be.

1.3 Development of SCC Mixes with and without Steel Fibers

Before adding the fine particles, the coarse aggregates were mixed together in the concrete mixer to make the trial mixes. After two minutes of mixing, the powdered ingredient was added. To improve the consistency and flow of the mixture, two-thirds of the SP was dissolved in water and then added back in [5]. A slump flow test for T50 was performed after the SCC was mixed. If separation and bleeding were readily apparent in the experimental mixes, they were discarded. This is how SCC mixtures came to be.

1.3.1 Test on Mortar

Flow cone tests and V-funnel testing were performed on motors using a range of water/powder ratios and SP dosages. Since adding the super plasticizer, the paste has taken on a new rheology. There was uniformity in the FA's subject matter. The projected slump flow height ranged from 24 to 26 centimetres. The duration of the V-funnel is around seven to 10 seconds. The slump flow at which the V-funnel becomes less than 7 seconds has been decreased the W/P ratio. Increasing the water-to-powder ratio yielded the desired slump flow and a V-funnel period of more than 11 seconds. In order to satisfy the aforementioned requirement, an investigation on the effects of varying SP dosages was conducted. When the required parameters weren't met, we had to tweak the cement and fly ash amounts.

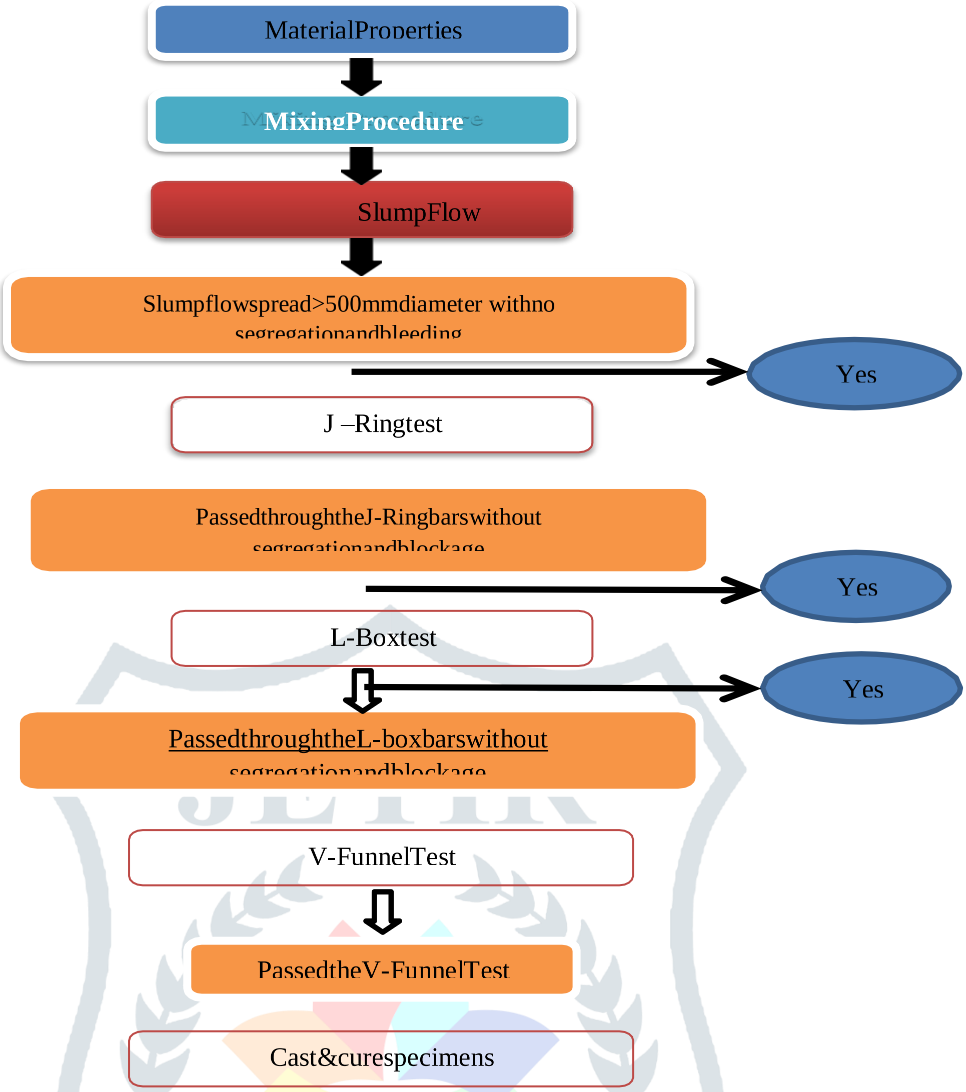

Figure1.1 Experimental program on Fresh state properties of SCC

1.4 test on beam-column joint

Beam column junction is where a beam and column meet. ACI 352R-02 a beam-column junction is the column section where the deepest beam crosses. BCJ includes corner, interior, and exterior joints. Concrete composition affects joint behavior. Severe earthquakes destroy joints. Using alternate component materials in concrete may affect the joint's performance.

1.4.1 Monolithic Concrete Structure of Beam-Column Joint

Loading requirements for the connection and projected deformations of the connected frame sections while resisting lateral loads are used to categorise beam-column connections in monolithic concrete structures into two classes, Type-1 and Type-2. Type-2 is a moment-resisting connection whose mechanical properties are preserved even when reversed into an inelastic range of behaviour, and Type-1 is a deformation-free inelastic connection described in this provision. Whether a beam-to-column junction is considered an interior, exterior, or corner connection is determined by the number of components making up the joint, as stated by ACI-352R.

1.4.2 Exterior Beam-Column Jointsand Critical Aspects of Joint Behavior

Some outer beam-column connections may become unstable when flat, multi-story frames are subjected to larger magnitudes of seismic stresses. The external activity of a joint and the corresponding internal pressures it creates are seen. Clearly, the shear panel zone of the joint generates both tensile and compressive stress along the joint's diagonal (fc and ft, respectively). Here are some thoughts on how stress might alter your health. T = tensile tension of the reinforcement, Cc = compressive force of the concrete, Cs = compressive force inside the reinforcement, and V = shear force; b and c denote the beam and column, respectively.

Figure 1.2 Types and location of beam-column joint

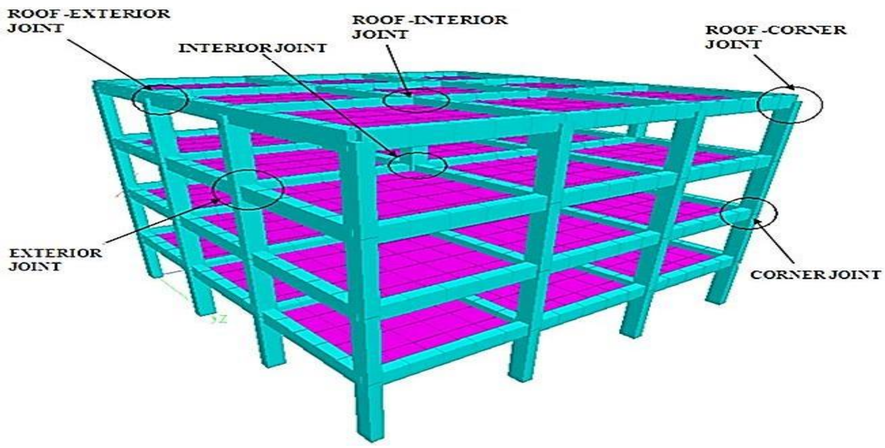

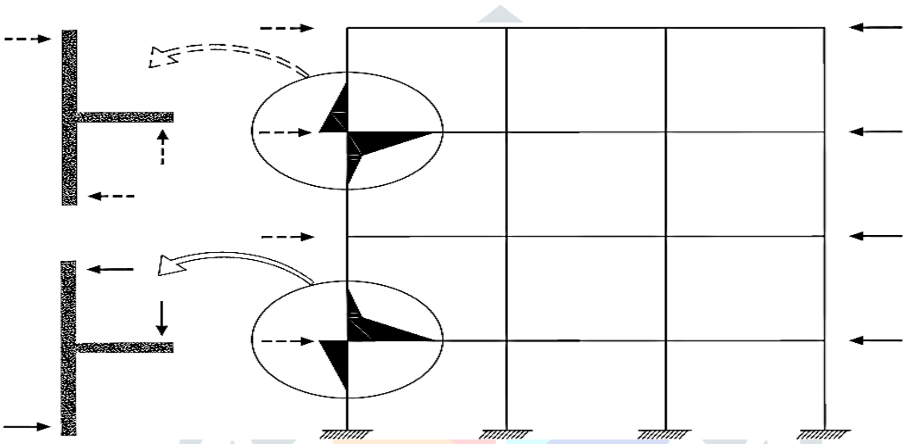

Figure 1.3 Actions at exterior beam-column joint on framed structure

1.5 Loading Arrangement

Every specimen was put through a static load test on a 100-ton loading frame. The column was under constant stress of 150 kN. The purpose of this was to prevent any rocking or wobbling of the column. Joint fractures occurred in every instance just after the yield load. Large numbers of tiny fractures appeared in steel FIBER reinforced beams [6]. Loading configurations of the successful Type A BCJ specimen and the failed specimen are shown in. A base cover was used to keep the specimen standing and completely isolated from any lateral movement. A 25-ton hydraulic jack was employed to provide constant force to the BCJ specimen's top throughout loading, keeping it rigid and in place. The Type A BCJ model has two dial gauges on each side. Dial gauge readings were taken after the weight was put on the specimen to reveal its degree of movement. Type B BCJ specimen loading configuration and damaged joint are shown in. Using a base cover, we were able to completely prevent the specimen from moving laterally while keeping it standing. A 25-ton hydraulic jack was utilised to provide a constant force to the top of the BCJ specimen during loading, ensuring that it would remain standing and still throughout the process [7]. Two dial gauges were employed to measure the resulting shifts in position when the specified loads were increased. Dial gauge readings were taken after the weight was put on the specimen to reveal its degree of movement. You can see the loading settings for the successful and unsuccessful Type C BCJ specimens. Using a base cover, we were able to completely prevent the specimen from moving laterally while keeping it standing. A 25-ton hydraulic jack was employed to provide constant force to the BCJ specimen's top throughout loading, keeping it rigid and in place. Two dial gauges were employed to measure the resulting shifts in position when the specified loads were increased. The displacements were calculated by comparing the corresponding numbers on the dial gauge after the specimen was loaded from one end alone.

1.6 Details of Specimens Subjected to Investigation

The details regarding the specimens categorized under TYPE A , TYPE B & TYPE C are given in(table1.1)

Table1.1 Specimen details

TYPE-A	tab–30%RBA
	B1–30%RBA+0.5%SF
	B2–30%RBA+0.75%SF
	B3–30%RBA+1.0%SF
TYPE-B	TBB–30%RBA
	D1–30%RBA+0.5%SF
	D2–30%RBA+0.75%SF
	D3–30%RBA+1.0%SF
TYPE-C	TCB–30%RBA
	F1–30%RBA+0.50%SF
	F2–30%RBA+0.75%SF
	F3–30%RBA+1.0%SF

1.7 Properties of Materials and Aggregate Blends

After being subjected to the required standard testing procedures, all of the SCC component materials were deemed suitable for use in the production of SCC. We observed that a ratio of 50:50 fine to coarse aggregate produced the maximum bulk density. This optimal ratio of fine aggregate to coarse aggregate was employed in the mix proportioning of SCC blends with decreased porosity. A 30% replacement of coarse aggregate with RBA was evaluated in the evaluation of SCC beam column joints since it was observed that using the RBA in larger proportion decreased the flow characteristics. Steel fibres at a weight of 1% were added to the cement mix to ensure that SCC's fluidity and durability would not be compromised.

1.7.1 Fresh State Tests on SCC

The initial part of the experiment was blending RBA and SF to find the ideal mix % of SCC, which would then have the right fluidity and viscosity for the application. The combination was modified to conform to SCC standards after additional state testing was completed [8]. Several FA and CA permutations helped achieve this goal. Slump flow, T50, J-ring, V-funnel, and L-box are some of the experiments that may be run. Table 1.1 of EFNARC 2002 details the prerequisites for new SCC features to be approved. Table 1.1 Acceptance criteria for fresh state tests on SCC

S. No.	Description of test	Unit	Typical values	
			Min	Max
1	Slump flow	mm	650	800
2	T_{50} Slump flow.	Sec	2	5
3	J-ring	mm	0	10
4	V-funnel.	Sec	6	12
5	L-box.	H_2/H_1	0.8	1.0

1.7.2 Slump Flow

The flow experiments (table 1.2) validate that SCC is up to the standards set out in the scholarly literature. As an additional matter of fact, the slump flow test is a reliable method for estimating the SCC flow characteristics. When test results were examined, it became clear that the flow spread was directly affected by the percentage of natural aggregate that was replaced with RBA. Results from experiments with samples M2, M3, and M4 demonstrated that, as the proportion of RBA replacement rose, the flow dispersion fell even lower. In addition, samples M5, M6, and M7 showed a decrease in flow spread after receiving injections of SF at concentrations of 0.5%, 0.75 %, and 1.0 %, respectively. EFNARC was successful in keeping the flow spread within the desired 650-800 mm range because to careful regulation of the SP dosage and a cap of 1% SF. (2002). Displays a comparison of the experimental slump flow. The maximum and lowest slump flow values as measured by EFNARC 2002 are shown. Table 1.2 displays the results of the slump flow test.

MIX ID	Slump flow	
	D (mm)	T_{500} (Sec)
NSCC	740	2
M2	731	2.18
M3	727	2.95
M4	723	3.05
M5	721	3.61
M6	716	3.85
M7	704	4.09

Table 1.2 Slump flow test result

1.7.3 T_{50cm} Flow Test

The following may be ascertained with the use of the results of the T50 cm flow test. There was a 50-centimeter height increase in around two seconds for the M1 trial mix that lacked RBA or SF. M2, M3, and M4 generated T50 cm values of 2.18, 2.95, and 3.61 seconds at 20%, 30%, and 40% RBA, respectively. When measured in centimetres, M5, M6, and M7 all hit T50 at 3.61, 3.85, and 4.09 inches, respectively. It can be demonstrated that when the RBA and SF percentages grew, the T50 cm decreased. The intended result for SCC was achieved, however, by adjusting the SP dosage. Also It is generally accepted that as the quantity of powder grows, so does the probability. When the powder concentration is too high, the paste becomes too viscous and cannot flow freely. This illustrates how the volume of the paste influences the physical properties of the SCC's fluidity. SCC's flow capability remained the same even after the FIBER was drastically lowered. Table 1.3 both provide T50 cm comparative values.

Table 1.3 T_{500} test result

MIX ID	T_{500} (Sec)
M1	2
M2	2.18
M3	2.95
M4	3.05
M5	3.61
M6	3.85
M7	4.09

1.7.4 L-Box Test

After ensuring the mixture would droop without breaking, an L-box test was conducted. The L-box test was used to analyse the void-filling and flow-through properties of the SCC mixes. Specifically, the test was designed to provide a result of 1 for the ratio H2/H1. The passing and flowing capacities of samples M2, M3, and M4 were quite similar to sample M1, with just minor differences. The steel FIBERs may have had a blocking impact on M5, M6, and M7, reducing their flow ability and transit ability. Any batches that bled or separated were discarded, and fresh ones were prepared. L-box test results are shown in table 1.4

Table 1.4 L-box test results

MIX ID	L-Box (mm)
M1	1.0
M2	0.95
M3	0.91
M4	0.89
M5	0.86
M6	0.84
M7	0.83

1.7.5 Comparison of V Funnel Test

After the experimental mixture passed the slump flow test, it was moved on to the V-funnel test. The V-funnel times of M2, M3, and M4 were all greater than those of M1. In addition, M5, M6, and M7 traffic took a long time to move through the It resembles a V-shaped funnel most closely. An increased proportion of RBA and Steel fibres in SCC reduces the passing ability of the blend, which in turn affects its ductility [9]. The required flow properties of SCC were achieved by a battery of experiments that included different ratios of RBA and Steel FIBERs. Any batches that bled or separated were discarded, and fresh ones were prepared. The V-funnel values obtained for the various mixes are compared and the V funnel time is provided in (table 1.5).

Table 1.5 V-funnel test results

MIX ID	V- Funnel (Sec)
M1	8.31
M2	8.96
M3	9.13
M4	9.47
M5	10.22
M6	10.89
M7	11.07

Segregation Resistance the ability to produce SCC with acceptable flow and passage properties requires a high level a defiance against discrimination. Throughout the course of the experimental investigation, any trial mixture that exhibited signs of segregation was discarded, and a new mixture was created. All seven optimal combinations were very resistant to segregation, whether they were derived from M1, M2, M3, M4, M5, or M7. SCC's mortar phase was also seen to have uniform distribution of aggregates and steel fibres. When the right amount of SP was added to the SCC formula, it stayed stable. Hardened state tests like compression test, split tension test and flexural strength test were conducted and the results are given in (table 1.6).

1.8 Compression Test

Compressive test findings show that when RBA replacement percentage rises in SCC, the material's strength decreases. It was seen in samples M2, M3, and M4. This is presumably due to RBA's relatively low crushing strength compared to that of other natural aggregates. Like M5, M6, and M7, the addition of steel FIBERs increased the material's compressive strength. The results from the tests are listed in Table 1.6, and a visual representation of the comparison can be seen in Figure 1.4.

Table 1.6 Hardened state test result

MIX ID	Hardened state test								
	Strength of compression (N/mm2)			(N/mm2) Flexural strength			Split tensile strength (N/mm²)		
	7th day	14th day	28th Day	7th day	14th day	28th day	7th day	14th day	28th day

M1	18.34	24.72	37.45	2.51	3.29	3.53	1.95	2.65	2.99
M2	17.75	21.12	34.32	2.34	2.56	3.24	1.88	2.43	2.85
M3	14.71	18.89	28.14	2.25	2.55	3.05	1.77	2.16	2.77
M4	11.32	15.56	25.61	2.2	2.85	2.86	1.68	2.06	2.66
M5	16.89	22.30	35.68	2.56	2.80	3.20	1.98	2.48	2.99
M6	16.76	20.24	30.14	2.42	2.78	3.35	1.88	2.25	2.94
M7	13.25	17.37	27.45	2.54	2.96	3.50	1.96	2.45	2.95

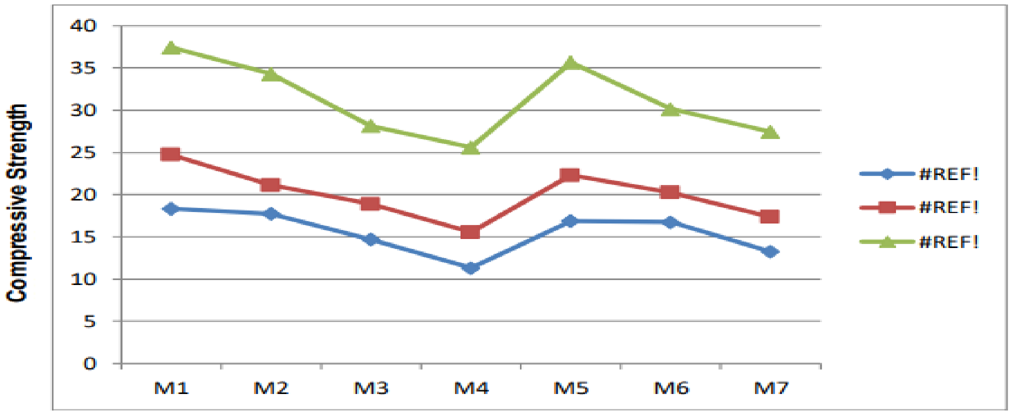

Figure 1.4 compressive strength Graph

0	M1	M2	M3	M4	M5	M6	M7
7 Day	18.34	17.75	14.71	11.32	16.89	16.76	13.25
14 Day	24.72	21.12	18.89	15.56	22.3	20.24	17.37
28 Day	37.45	34.32	28.14	25.61	35.68	30.14	27.45

1.9 Split Tensile Strength

Steel FIBER improved tensile strength upon splitting. RBA's lower split tensile strength is compensated for by the use of steel FIBERs. The RBA-infected samples failed as a group as a whole. However, by limiting the replacement percentage of the RBA, a significant improvement in split tensile strength was accomplished [10]. Results from the split tensile strength test and a comparison chart are shown in tables (table 1.6) and (Figure 1.7).

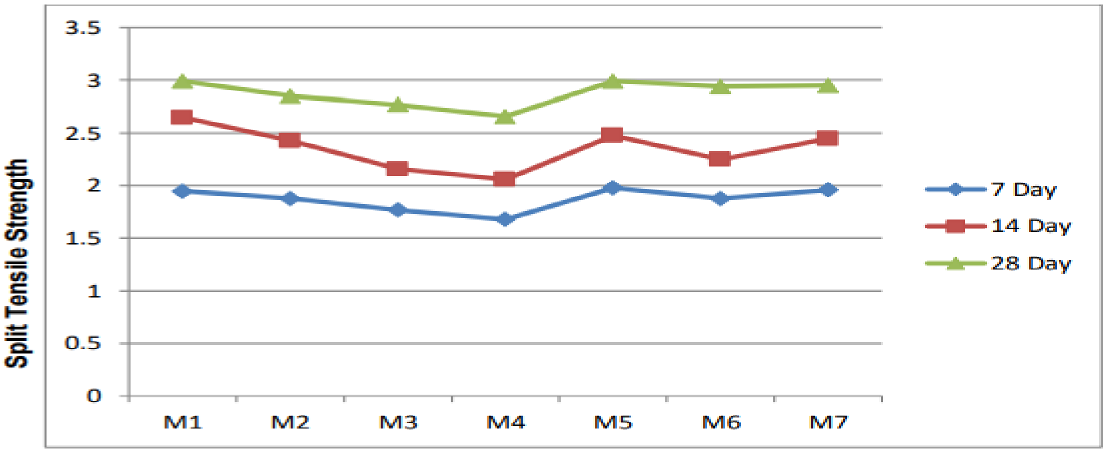

Figure 1.5 Comparison of split tensile strength

0	M1	M2	M3	M4	M5	M6	M7
7 Day	1.95	1.88	1.77	1.68	1.98	1.88	1.96
14 Day	2.65	2.43	2.16	2.06	2.48	2.25	2.45
28 Day	2.99	2.85	2.77	2.66	2.99	2.94	2.95

1.9.2 Flexural Strength Test

The inclusion of steel fiber reinforcement enhanced the split tensile strength of SCC in specimens M5, M6, and M7 This is because the steel fibers provide the beam pliability. From this it is obvious that the negative qualities RBA might be mitigated by making use of utilization of steel fibers in SCC. table 1.6 and Figure 1.6 illustrate the results and flexure strength comparisons, respectively.

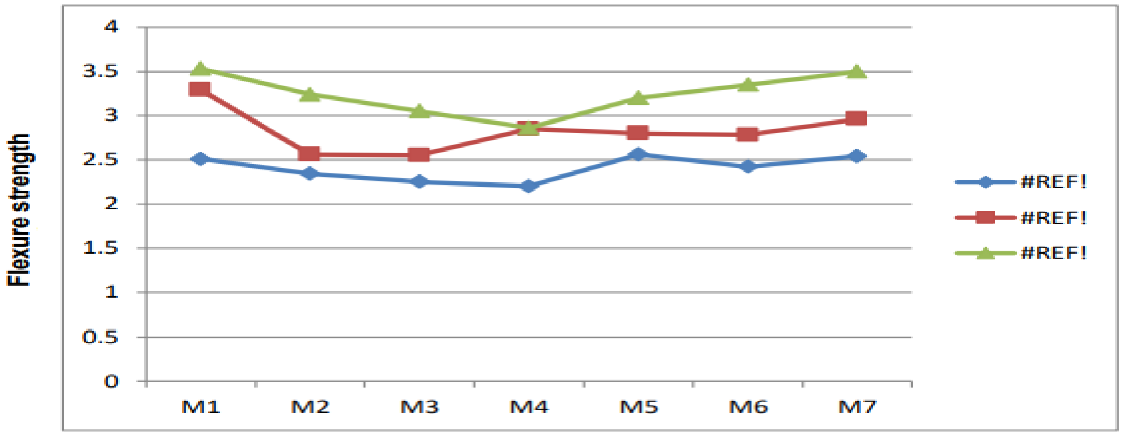

Figure 1.6 Comparison of Flexural strength

0	M1	M2	M3	M4	M5	M6	M7
Series1	2.51	2.34	2.25	2.2	2.56	2.42	2.54
Series2	3.29	2.56	2.55	2.85	2.8	2.78	2.96
Series3	3.53	3.24	3.05	2.86	3.2	3.35	3.5

GENERAL BEHAVIOUR AND FAILURE MECHANISMS

1.10 Cracking Pattern and Failure Mode

All joints exhibited severe cracking at roughly 5mm displacement. The joint defects widened, causing concrete spelling (particularly in the concrete cover zone) and finally exposing the steel reinforcing bars. Tensile fractures formed in virtually all specimens at the column-beam contact. The inclusion of steel FIBERs in specimens M5, M6 and M7 reduced the fracture width. The specimens failed owing to increased fracture width at the beam-column junction. All of the specimens had a distinct vertical cleavage. The crack pattern shows that the crack width decreases with the addition of steel FIBERs. The fracture width reduces as the steel FIBER content increases.

1.10.1 Displacement Ductility

The ratio of the final displacement to the yield displacement is what's meant to be understood when speaking of the "displacement ductility factor."

Table 1.8 Displacement Ductility Factors of Concrete Specimens

S.No	Specimen Id	*u* mm	*y* Mm	Displacement Ductility Factor
1	A1	48.66	5.82	8.36
2	A2	35.48	4.68	7.58
3	B1	38.21	4.96	7.70

4	B2	40.37	5.35	7.55
5	B3	42.94	5.42	7.92
6	C1	24.33	2.91	8.36
7	C2	18.28	3.71	4.93
8	D1	20.44	3.43	5.96
9	D2	21.37	3.29	6.50
10	D3	22.18	3.1	7.15
11	E1	23.14	2.86	8.09
12	E2	17.38	3.88	4.48
13	F1	18.62	3.68	5.06
14	F2	19.85	3.24	6.13
15	F3	21.78	2.84	7.67

From the table 1.8 we know in Type A specimen that the ductility calculated for tab specimen is 8.36. For tab specimen the ductility value is

	A1	A2	B1	B2	B3
TYPE A JOINT	8.26	7.58	7.7	7.85	7.92

Displacement ductility of Type A joint

7.58 which is 10% less than that of tab. However the ductility of TAFI, B2 & B3 have a ductility factor of 7.58, 7.70 & 7.92 which is in increasing order. Ductility of the joint is appreciably increased due to the addition of steel FIBERs to the BCJ. Similar is the case with Type B and Type C specimens. The comparison chart for the displacement ductility.

	C1	C2	D1	D2	D3
Type B	8.36	4.93	5.96	6.5	7.15

Displacement ductility of Type B joint

	E1	E2	F1	F2	F3
TYPEC JOINT	8.09	4.48	5.06	6.13	7.67

Displacement ductility of Type C joint

1.10.2 Stiffness Behavior

When stress is applied to a reinforced concrete beam-column junction , the joint's stiffness decreases. The following factors have contributed to the decrease in stiffness. Concrete and steel are loaded and unloaded during the loading process. As a result, the fatigue limit of the materials will be exceeded, causing micro-cracks in the joint. This results in a decrease in the stiffness of the joints as a consequence of the increased deformations. This means that the deterioration of stiffness at the beam-column joints exposed to loads has to be evaluated .table 1.9 gives the stiffness value and the comparison respectively.

Table 1.9 Stiffness calculation

Specimen /Groups	Yielding displacement in mm- δ_y	Ultimate load in kN -P_u	Ultimate displacement in mm δ_u	
tab	4.82	42.4	48.66	8.80
tab	7.68	37.4	35.48	4.87
B1	6.23	38.5	38.21	6.18
B2	5.35	39.2	40.37	7.33
B3	5.2	40.2	42.94	7.73
TBN	2.91	19.5	24.33	6.70
TBB	3.71	15.2	18.28	4.10
D1	3.43	16.3	20.44	4.75
D2	3.29	16.8	21.37	5.11
D3	3.1	17.1	22.18	5.52
TCN	2.86	18	23.14	6.29
TCB	3.88	13.2	17.38	3.40
F1	3.68	15.5	18.62	4.21
F2	3.24	15.8	19.85	4.88
F3	2.84	16.1	21.78	5.67

From the table 1.9 it is evident that for Type a specimens tab has a stiffness of 8.80 and tab has a stiffness of 4.87. The stiffness of B1, B2 &B3 are 6.18, 7.33 and 7.73 respectively. It is clear that the specimen with RBA exhibited stiffness degradation. However the addition of steel fibers improved the same. Similar is the case with Type B and Type C specimens.

ID	TA	TA	TAF	TAF	TAF
TYPE A	8.8	4.8	6.1	7.3	7.7

Stiffness of Type A joint

ID	TB	TB	TBF	TBF	TBF
TYPE B	6.7	4.1	4.7	5.1	5.5

Stiffness of Type B joint

ID	TC	TC	TCF	TCF	TCF
TYPE C	6.2	3.4	4.2	4.8	5.6

Stiffness of Type C joint

The testing is load regulated. The specimens were tested until they reached their maximum failure capacity as indicated. First cycle with 1 tone weight showed no fractures. During the second cycle, with a 2 tone load, flexural fractures appeared at the beam-column junction. The loading method is repeated until the full ultimate loading capacity is attained. Tensile pressures caused broad open fractures and diagonal fissures in several beam-column assemblages. Others test assemblies had spelled joint core concrete owing to compressive stress, while some had shear fractures in the column. The RBA specimens had a wider fracture than the non-RBA counterparts. Steel fibers added to BCJ specimens significantly decreased fracture width. Fine cracks were seen in the joint area. The steel fibers promote ductility and decrease stiffness of the joint.

1.11 Conclusion

In this study, we look at experimental research on the impact of RBA and steel fibres used in beam-column junctions on SCC behaviour. The purpose of this research was to provide a starting point for optimising the percentages of recycled brick aggregates and steel fibres used in SCC mixes. To achieve this goal, many SCC mix combinations were developed using different percentages of the component ingredients, and their fresh state properties were compared. Finally, hardness tests on SCC specimens were conducted in order to assess the strength qualities up until the needed SCC properties were obtained by the optimal mix%. Understanding the behaviour of SCC beam column junctions required a close examination of three distinct kinds of beam column joint specimens, which were discussed in Chapter 4. Results and discussion of the experiments are presented here. This study examined the production and erection procedures, fixing arrangement details, and experimental setup of the reinforced concrete beam-column joints test specimen with distinct measurement arrangements and testing processes. The resources used in this study include qualities like being easy to understand. In this study, we categorise the beam-column junction assemblages into three groups, each with three examples.

References

1. Nitesh, K. J. N. S., Rao, S. V., & Kumar, P. R. (2019). An experimental investigation on torsional behaviour of recycled aggregate based steel fiber reinforced self compacting concrete. Journal of Building Engineering, 22, 242–251. doi:10.1016/j.jobe.2018.12.011
2. G. S. Pandit and S. P. Gupta, “Torsion in concrete structures” 1st edition, CBS publishers and distributers.
3. Chengdong Su, Haixiao Lin (2017) Mechanical performances of steel fiber reinforced high strength concrete disc under cyclic loading. Construction and Building Materials, (146): 276-282.
4. Biao Li, Lihua Xu, Yin Chi, Biao Huang, Changning Li (2017) Experimental investigation on the stress-strain behavior of steel fiber reinforced concrete subjected to uniaxial cyclic compression. Construction and Building Materials, (140), 109-118.
5. Oldrich Sucharda, Malgorzata Pajak, Tomasz Ponikiewski, Petr Konecny (2017), Identification of mechanical and fracture properties of self-compacting concrete beams with different types of steel fibers using inverse analysis. Construction and Building Materials, (138) 263-275.
6. Reddy, C.S., Sai, K.R. and Kumar, P.R., (2013). “Mechanical and Durability properties of Self Compacting Concrete with recycled concrete aggregates”. Contributory Papers, 255.
7. Su, N., Hsu, K. C., & Chai, H. W. (2001). A simple mix design method for selfcompacting concrete. Cement and concrete research, 31(12), 1799-1807.
8. Concrete, S. C. (2005). The European Guidelines for Self-Compacting Concrete.
9. Bouzoubaa, N., & Lachemi, M. (2001). Self-compacting concrete incorporating high volumes of class F fly ash: Preliminary results. Cement and concrete research, 31(3), 413-420
10. Najim, K. B., Saeb, A., & Al-Azzawi, Z. (2018). Structural behaviour and fracture energy of recycled steel fibre self-compacting reinforced concrete beams. Journal of Building Engineering, 17, 174-182.